國立雲林科技大學
96學年度博士班招生入學考試試題

所別：化學工程與材料工程系
科目：科技文獻

一、 請針對附件一內容，提供簡短閱讀心得。(20%)

二、 請針對附件二內容，回答下列問題。

1. 請概略描述“hybrid energy system”組成方式。(15%)

2. 依個人經驗判斷作者提供“hybrid energy system”構想是否可以在台灣實現？(15%)

三、 請針對附件三內容，回答下列問題。

1. 本篇論文的研究目的。(10%)

2. 本篇論文的研究方法。(20%)

3. 本篇論文的具體貢獻。(20%)

Perspective (附件一)

Future of U.S. Research Universities in a Globalized World: A Chemical Engineer's View from Singapore

W. R. Schowalter
Dept. of Chemical Engineering, Princeton University, Princeton, NJ 08544

DOI 10.1002/aic.10950
Published online July 25, 2006 in Wiley InterScience (www.interscience.wiley.com).
Keywords: research university, globalization, graduate education, competitiveness

Introduction

The forces of globalization have been with us for a sufficiently long time so that eyebrows are no longer raised when statements such as, "Globalization is the 21st century equivalent of the Industrial Revolution" are made. Nearly every human endeavor has been affected by forces described in Thomas Friedman's "The World is Flat"[1]. Examples include the response we get to toll-free help calls as well as factory closings caused by the need for a corporation to manufacture components abroad in order to remain competitive.

In contrast to the tectonic-plate scale of rearrangements seen in the manufacturing and service industries, operation of the major U.S. research universities has proceeded without corresponding upheavals. Why is this? Should we expect something different? What does the future hold for us? In this article, I shall provide some opinions regarding these and other questions. Because my own international interests in recent years have been focused on Asia my comments are Asia-centric, and they reflect my experiences as senior advisor to the president of the National University of Singapore (NUS).

Anomalous Culture of the Research University. Audacious Discoveries Emanating from Citadels of Conservatism

Those research universities generally acknowledged to be among the best in the world, house faculties whose professional reputations are garnered by upsetting conventional wisdom in order to make new discoveries or to establish new paradigms. Yet corporately they belong to a group considered to be resistant to structural change at a level possibly comparable to most organized religions. Indeed, a case can be made that such resistance to change is a factor supporting the longevity of these institutions. However, permanence is not synonymous with excellence. The purpose of this article is to ask whether that resistance to change will hold the universities largely impervious to globalization and, if so, whether U.S. universities will retain their positions of prominence. My opinion is that unless U.S. universities embrace globalization as a new opportunity, they will, within a generation, find themselves among the also-rans of the world's research universities.

Context

In 2003 Goldman Sachs[2] published a scenario in which, by the year 2050, Asia could dominate the world's economic landscape. China would have the highest gross domestic product (GDP) among all nations, followed by the U.S. and India, respectively (Figure 1). Evidence that the stirring Asian giants are already affecting the academic research landscape is not hard to find. An example is found in our own flagship research publication, the *AIChE Journal*. Table 1 shows the origin of articles published during the first five months, respectively, of 1990, 1995, 2000, 2005, and 2006. Two interesting results emerge from this simple sampling. First, *AIChE Journal* has been a truly international journal for a long time, and it is now dominated by articles from abroad. Second, the number of articles from China and India is growing rapidly, both in absolute terms and relative to the total number of articles published.

Is the Pipeline of Talent to the U.S. Likely to Run Dry?

It is well known that graduate research in engineering and science in the U.S. is fueled by students from abroad, with well over 50% of our graduate students coming from other countries. Is this flow of talent likely to cease? I do not think so. However, I do believe that, barring major political upheavals, our ability to attract top students from abroad will be severely tested within the next decade, and I offer several observations to support that claim.

W. R. Schowalter's e-mail address is schowalt@princeton.edu.

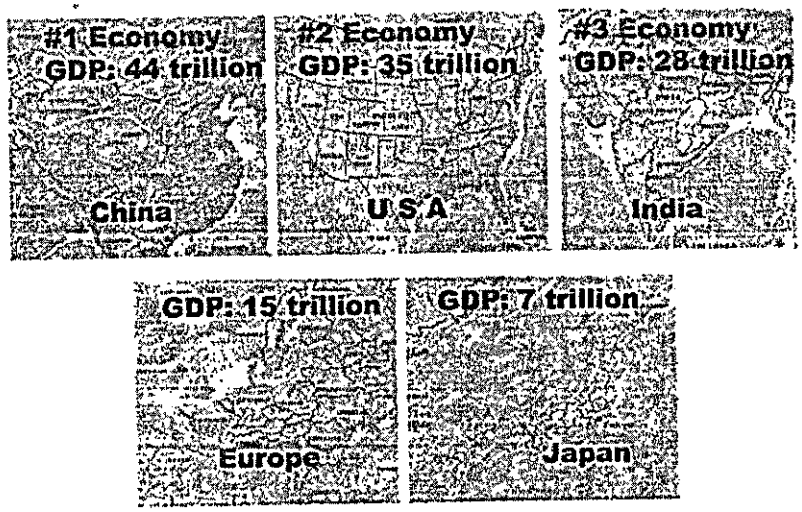

Figure 1. Goldman Sachs[2] scenario of countries with the largest Gross Domestic Products (GDP) in 2050 (courtesy National University of Singapore)

History

Well into the 20th century, it was common for American scientists to spend time under the tutelage of a mentor in Europe. This was also true for several of the early giants of the chemical engineering profession.[3] That trend abated, and following World War II the center of the academic universe became the U.S. We have enjoyed that hegemony for so long that most of us have known no other condition. To us, it is "normal". However, with the flattening force of globalization at work, it is important to recognize that our present state is as abnormal as it is for the world's automobile appetite to be satisfied by three manufacturers headquartered in Detroit.

Knowledge is (economic) power

There is ample evidence to show that just as iron, coal, and oil have been central to manufacturing prowess, knowledge.— and its application — are raw materials for growth in the late 20th and early 21st centuries. The special edition of *Newsweek*[4] coinciding with the 2006 World Economic Forum in Davos, Switzerland, was titled "The Knowledge Revolution. Why Victory Will Go to the Smartest Nations and Companies". Articles by Bill Gates, Tony Blair, and others have titles, such as "Ideas Matter", "Failing Europe" and "Where America Stands".

The issue is a chilling read for those who believe the United States (or Europe) will house the world's engines of growth through the 21st century.

Rise of Asia.

I have already referred to the expected rise of Asia to economic primacy within the next few decades. Alongside these figures is the less quantifiable, but equally important expectation among Asians that they are the wave of the future. In Shanghai, Singapore, and parts of Bangalore, the expectation is evident. It is a different environment than one senses in the U.S. or Europe. One way to convey the Asian sense of resolve and anticipation is to quote from an article written by Singapore's prime minister, Lee Hsien Loong, in the aforementioned *Newsweek* edition. He wrote, "On an intelligent island, every pair of hands has to be a pair of thinking hands", and "Globalization will force nations to reallocate resources, restructure their economies and reorient their societies for the future. Singapore accepts this as a given".

Timescale of change

Another characteristic of modern civilization about which much has been written is the shrinking timescale over which significant change occurs. One instructive way to illustrate this is to note the rank-ordered list of the largest corporations at five-year intervals during the past 30 years. The increasing volatility of that list is apparent. Applying that exercise to the academic scene and using some measure of graduate-study quality in engineering and science, the corresponding list will show far less volatility. However, perceptions of research quality do change, and I believe they are now changing more

Table 1. Papers Published in *AIChE Journal* During the First Five Months of Selected Years*

Year	1990	1995	2000	2005	2006
% Foreign Papers,	36	36	51	56	65
% from China and India	5	3	4	9	9
% from China and India among Foreign Papers	12	8	8	17	13
Number of papers from China & India	4	4	4	13	16
Total Number of Papers	88	139	103	137	184

* In cases where coauthors were from the U.S. and from abroad, assignment was based on some combination of the location at which the work was performed and the source of its support.

國立雲林科技大學
96 學年度博士班招生入學考試試題

所別：化學工程與材料工程系
科目：科技文獻

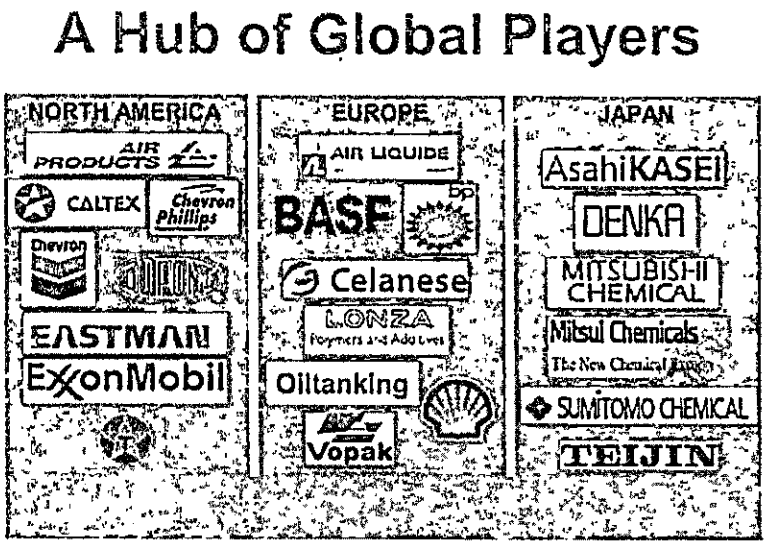

Figure 2. Recent occupants of Jurong Island (courtesy Singapore Economic Development Board).

rapidly than at any time in memory. Does this spell the demise of U.S. research universities? I do not think it does. What I believe will change in the next decade is the near-monopoly the U.S. has had in recruiting the best students for PhD and post-PhD education. Graduate students and post-docs will have more options. There will be more universities competing in the global talent reservoir, and the U.S. will face more than token competition, particularly from Asian universities. The increased competition will occur not only at the student level, but also for talented faculty members — at all levels. This change is, in my opinion, inevitable. It would be both unrealistic and unwise to ignore it or to attempt to prevent it. The balance of this article will focus on how we, and indeed the global academic research enterprise, can profit from these trends.

Some Observations

Increasing global talent base

Both China and India have ambitious plans to upgrade advanced education in engineering and science. This includes making those curricula available to a larger fraction of the population. Given a huge population base of over two billion people, a small increase in the fraction of talented young people pursuing research careers will result in very large changes in the global talent pool. It will be important to U.S. universities to have access to this pool, and to provide competitively attractive means to do so. The waning interest and performance of U.S. students in quantitative subjects is well known. With more than half of our country's graduate-student population already coming from abroad, an even greater disconnect is likely between U.S. graduate education in science and engineering and the U.S. population as a whole.

Stay close to the customer

There is every reason to expect that along with Asia's increasing capacity for producing a technically educated work force, jobs requiring such skills will also increase. In the chemical and petroleum industries this has already happened in manufacturing. The position on the value chain of biotechnology and some areas of electronics is rising, and research and development (R&D) opportunities are expanding. A few years ago a major U.S. pharmaceutical company opened a research laboratory in Singapore. One of the executives associated with the decision said, "Why should we bring people from Asia to the U.S., train them, and then go through the requirements necessary to keep them here? We should provide jobs for them near their homeland so they do not have to leave it." If this seems obvious to the corporate sector, should it be any less so for academe? The customers of a research university are, on the one hand, students; on the other, they are the corporations and universities to which our students are attracted after termination of their formal study. Should we not serve both of these customer bases by being in close proximity to them?

Singapore approach

As the major countries of the world attempt to cope with globalization, they may find instructive the approach of the tiny city-state that is Singapore. An island of less than 300 square miles with a population of four million, Singapore has contended with "globalization" since its founding as a trading port. The notion of adding value to goods that pass through it has now been extended to the flow of ideas. Singapore's location and size define a unique set of conditions, and to the extent that there is a "Singapore story" it will not serve as a template transferable to other nations. Nonetheless, there are important lessons to be learned from the Singapore experience.

In the 1980s Singapore determined that the chemical and petroleum industries were key drivers of its economy. To anchor the industry already present in the form of several refineries and manufacturing plants, and to attract others, the country embarked on a bold ($4 billion) project to co-locate components of that sector together on the fusion of several islands into one 12-square-mile complex known as Jurong Island. Utility and other infrastructure support were supplied centrally to Jurong Island's tenants. Recent corporate occupants are shown in Figure 2.

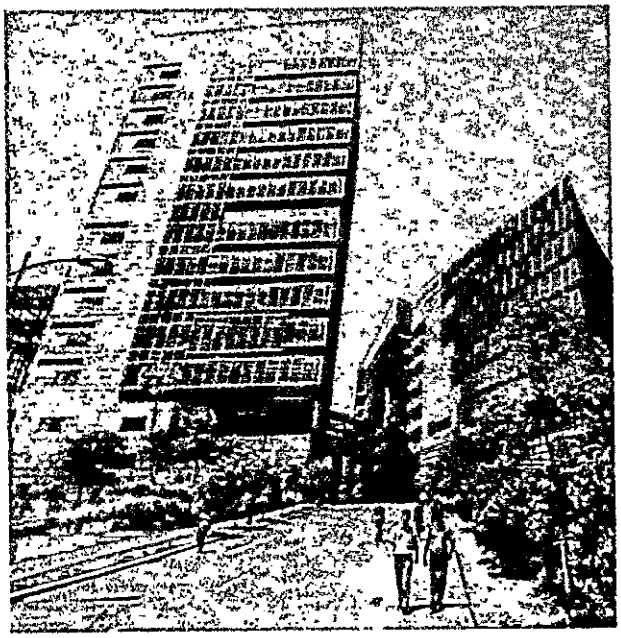

Figure 3. Two buildings of the Biopolis complex (photo courtesy of Singapore A*STAR).

It was recognized early on that R&D support should be available to this sector, providing means for companies to undertake, jointly or singly, R&D projects without encumbering the home R&D facilities. On the Singapore side this translated into a move toward an indigenous knowledge-based activity, an ingredient necessary to thrive in a globalized environment. Thus, in 2004, a government-sponsored Institute of Chemical and Engineering Sciences (ICES) was established on Jurong Island, with 34,000 square feet of laboratory space, and a current staff of more than 120 research scientists and engineers.

With Jurong Island a reality, the government, through its Agency for Science Technology and Research (A*STAR) expanded this model to the life sciences, but now with a larger emphasis on R&D, although still connected with present or perceived future manufacturing capacity. The result is a huge complex known as Biopolis (Figure 3). With the emphasis on ideas and research, Biopolis is a collection of A*STAR-sponsored research institutes (RI's) designed to resonate with the biotech and pharmaceutical industries. Nestled with these RI's are several corporate pharmaceutical laboratories, including firms such as Novartis and GlaxoSmithKline. Investment in the construction of Biopolis exceeded $300 million. However, the plan is not complete. The next phase is construction of a neighboring Fusionpolis, which will collect in contiguous space most of the RI's focused on physical science and engineering. This plan recognizes that the life and physical sciences form a continuum and must be synergistic[5].

Biopolis and Fusionpolis are in close proximity to the NUS campus in order to facilitate the link that should exist between advanced (PhD and post-PhD) education and the needs of the Singapore economy. For example, the research of several NUS PhD chemical engineering candidates takes place in ICES laboratories, and is conducted under the direction of chemical engineering faculty members who also hold ICES appointments.

What are the exportable lessons to be learned from the Singapore story that will help other countries to cope with globalization? Three are particularly important:

1. National resolve is a requirement.
2. Ideas are as much a raw material as are coal and iron. One can profit by adding value to ideas.
3. Ideas come from people, and those people are a valuable asset. They must be acquired by successful competition in an increasingly global marketplace.

Using Globalization to Enrich Research Universities

It should be understood that I am referring to institutional, not individual, responses to globalization. Individual faculty members have collaborated with like-minded colleagues abroad for as long as means of travel and communication have existed. However, the globalized environment in which we now find ourselves argues for institutional strategies that will not only prevent damage to U.S. and other western universities, but will allow them to thrive in a globalized society.

One can codify institutional responses into three broad categories, each with its advantages and pitfalls. Although each may, at first blush, appear self-evident, there are important policy questions that for the most part have not yet been satisfactorily addressed.

Branch campuses abroad

In the engineering arena perhaps the most visible example of this approach has been the experience of Georgia Tech in France (http://www.georgiatech-metz.fr). Since 1990 Georgia Tech has maintained a campus in Metz, in the Lorraine region of France. Established originally as a base for undergraduates wishing a study-abroad experience, the program has grown to the point where graduate degrees are offered in selected engineering disciplines, and collaborative research programs have been formed with several European Union universities. Georgia Tech Lorraine now has aspects of all three models described here.

A clear advantage of the branch campus model is the degree of control maintained by the home institution. However, this very fact implies a lack of parity with organizations and individuals in the host country. It is difficult to avoid perceptions of colonialism; and competition rather than collaboration with local institutions can occur.

Alliances

These are bilateral (or perhaps larger) memoranda of understanding (MOU's) between institutions, where each party perceives a clear advantage to collaboration. Typically, both instruction and research collaboration are incorporated into the MOU. The files of university presidents are filled with MOU's, but because of unrealistic expectations and insufficient mutual commitment, only a small fraction of these agreements has had a meaningful impact on the participating institutions.

(附件二)

Simulation of a small wind fuel cell hybrid energy system

M.T. Iqbal *

Faculty of Engineering, MUN, St John's, NF, Canada A1B3X5

Received 28 May 2002; accepted 11 June 2002

Abstract

This paper describes simulation results of a small 500 W wind fuel cell hybrid energy system. The system consists of a Southwest Wind Power Inc. AIR 403 wind turbine, a Proton Exchange Membrane Fuel Cell (PEMFC) and an electrolyzer. Dynamic modeling of various components of this small isolated system is presented. Simulink is used for the dynamic simulation of this nonlinear 48 V hybrid energy system. Transient responses of the system to a step change in the load current and wind speed in a number of possible situations are presented. Analysis of simulation results and limitations of a wind fuel cell hybrid energy system are discussed.

Keywords: Hybrid energy systems; Wind energy; Fuel cell; Dynamics of energy system; Simulation and control; Distributed power generation

1. Introduction

After many technological advances Proton Exchange Membrane Fuel Cells (PEMFCs) technology has now reached test and demonstration phase [1]. The recent commercial availability of small PEMFC units has created many new opportunities to design hybrid energy systems for remote applications. For example Hpower.com stationary power unit EPAC500 is a 500 W hydrogen fueled PEMFC for backup power in homes. Other examples of commercially available 500 W PEMFC includes

* Tel.: +1-709-737-8934.
E-mail address: tariq@engr.mun.ca (M.T. Iqbal).

0960-1481/03/$ - see front matter © 2002 Elsevier Science Ltd. All rights reserved.
PII: S0960-1481(02)00070-8

SR-12 from Avistalabs.com and HyPORT power generator from Hydrogenics.com. Such commercially available fuel cell units can be combined with other renewable energy sources such as wind energy. Production of hydrogen using energy from a wind turbine for later use in a fuel cell is being studied at the Hydrogen Research Institute [2]. A detailed study [3] done for the Department of Energy indicates that a wind fuel cell based integrated system will produce power at a much lower cost and will contribute a much lower amount of CO_2 to the environment. An experimental study of daily variations in the bus bar voltage of a hybrid energy system consisting of solar panels, wind turbine, fuel cells and batteries has been recently completed at the Desert Research Institute [4]. Many aspects of such a hybrid energy system need to be investigated e.g. cost, efficiency, reliability, and dynamic response of the electrolyzer, fuel cell and hydrogen storage components. One important aspect of a wind fuel cell hybrid energy system that needs further investigation is design and simulation of the control system. A block diagram of the hybrid energy system is shown in Fig. 1. The load can be supplied from the wind turbine and/or fuel cell. If the wind turbine is producing enough power, the load will be supplied entirely from wind energy. In case of low wind a share of power can be supplied from the fuel cell. If the output power from the wind turbine exceeds the demand, the excess power may be used to produce hydrogen for later use in the fuel cell. Most of the time, in this system, the fuel cell stack is to be operated in the variable current output mode. While in most applications fuel cells are operated at a constant current. A wind fuel cell hybrid energy system may be based on a reversible fuel cell system [5,6]. Reversible fuel cells are still not commercially available. Therefore, in this study a more practical fuel cell and an electrolyzer-based system is considered. The system description, modeling, Simulink based simulation and an analysis of system dynamics are presented below.

2. Description of the system

The system consists of a Southwest Wind Power Inc. AIR 403 wind turbine, a Proton Exchange Membrane Fuel Cell (PEMFC) such as Hpower.com EPAC500, an electrolyzer (www.stuartenergy.com), a wind mast, a dump load, a personal computer

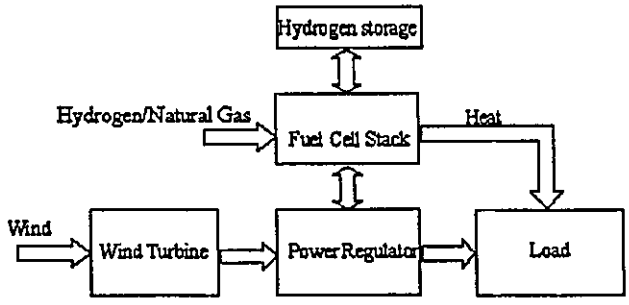

Fig. 1. Wind fuel cell hybrid energy system.

acting as controller and data acquisition system. Fig. 2 shows the details of system interconnections. For the study and analysis of the system the following parameters of this 48 V hybrid energy system are recorded: (a) Wind speed; (b) wind turbine current; (c) fuel cell voltage; (d) fuel cell current; (e) fuel cell temperature; (f) fuel cell pressure; (g) fuel flow rate; (h) wind direction; and (j) load current. The inbuilt wind turbine controller runs the turbine in variable speed mode while extracting maximum power. Fuel cell system consists of a PEM fuel cell stack and an electrolyzer. A fuel cell stack consists of 65 individual fuel cells connected in series. The output current can vary between 0 and 25 A. Fuel cell delivers the current difference between the load current and the wind turbine current. If the output voltage of the fuel cell stack drops below 46 V its controller switches on. A PC based PID type fuel cell controller adjusts the fuel and oxygen flow rates to maintain a constant stack output voltage. Controller action compensates the drop in the fuel cell stack voltage caused by the load current variations. If the wind turbine generates more current than required by the load then the excess current is diverted towards an electrolyzer. The electrolyzer-produced hydrogen is stored in a tank for later use in the fuel cell stack.

3. System model

The main components of the system are wind turbine, fuel cell stack, electrolyzer and controller. A standard classical method of representing the system by a set of differential equations and PID controller by a transfer function is used [7]. **Wind turbine** rotor diameter is 1.14 m. This self-regulating permanent magnet alternator based variable speed wind turbine produces 400 W at a wind speed of 12.5 m/s. Self-regulation (stall controlled) is achieved by the twisting of the blades. A wind

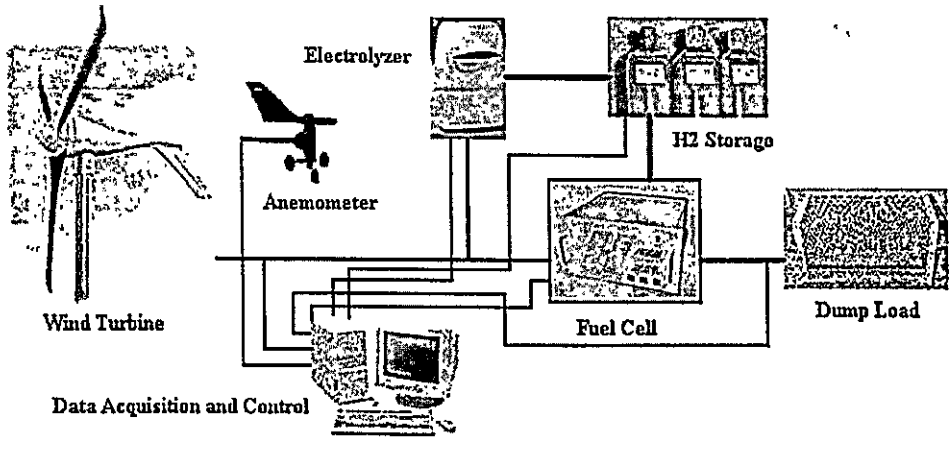

Fig. 2. Proposed wind fuel cell hybrid energy system.

turbine power curve is shown in Fig. 3. This small wind turbine is capable of extracting maximum power until a wind speed of 40 mph. Above a wind speed of 40 mph (17.9 m/s) the wind turbine quickly enters stall mode by blades twisting avoiding any over speed. This small wind turbine is well suited for roof top installation. Power curve of this wind turbine is nonlinear. It is digitized and the resulting table is used for simulation. Dynamics of the wind turbine are added by considering the wind turbine response as a second order slightly under damped system [7]. This is true when we take a first order moment of inertia (J) and friction based dynamic model for the wind turbine rotor and a first order model for the permanent magnet generator. Using this simple approach wind turbine dynamics are modelled as [7].

$$Y(s)/X(s) = 1/(s^2 + s + 1) \quad (1)$$

Where input is power obtained from the power curve for a known wind speed and output is actual power of the wind turbine.

Fuel cells are electrochemical devices that convert the chemical energy of a reaction directly into electrical energy. The basic building block of a fuel cell consists of an electrolyte layer in contact with a porous anode and cathode on either side. A schematic representation of a fuel cell with the reactant/product gases and the ion conduction flow directions through the cell is shown in Fig. 4 [8]. In a typical fuel cell, gaseous fuels are fed continuously to the anode (negative electrode) compartment and an oxidant (i.e. oxygen from air) is fed continuously to the cathode (positive electrode) compartment; the electrochemical reactions take place at the electrodes to produce an electric current. Fuel cells are classified by the type of electrolyte used in the cells and includes: (1) proton exchange membrane (polymer) electrolyte fuel cell (PEMPC); (2) alkaline fuel cell (AFC); (3) phosphoric acid fuel cell (PAFC); (4) molten carbonate fuel cell (MCPC); and (5) solid oxide fuel cell (SOFC).

These fuel cells are listed in the order of approximate operating temperature, ranging from −80°C for PEMFC to 1000°C for SOFC. Fuel cells can operate on natural gas/propane using a reformer. PEMFC running on hydrogen for stationary and portable applications are commercially available from a number of sources [1]. A number

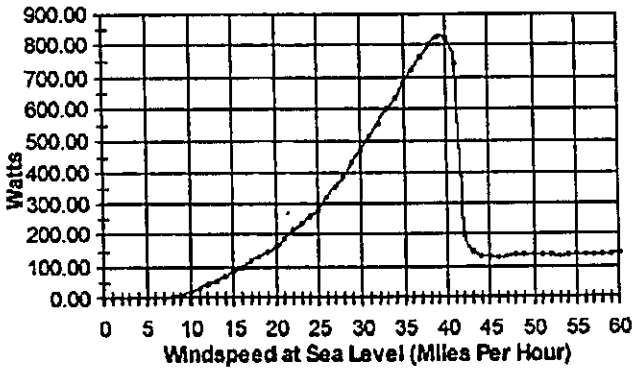

Fig. 3. Wind turbine power curve.

Available online at www.sciencedirect.com
ScienceDirect
(附件三)
ELSEVIER
Microporous and Mesoporous Materials 99 (2007) 30–36
MICROPOROUS AND MESOPOROUS MATERIALS
www.elsevier.com/locate/micromeso

SiO_2 nanotubes with nanodispersed Pt in the walls

Claus H. Rüscher [a], Inga Bannat [b], Armin Feldhoff [b], Lirong Ren [b], Michael Wark [b,*]

[a] *Institut für Mineralogie, ZfM, Leibniz Universität Hannover, Welfengarten 1, 30167 Hannover, Germany*
[b] *Institut für Physikalische Chemie und Elektrochemie, ZfM, Leibniz Universität Hannover, Callinstr. 3-3a, D-30167 Hannover, Germany*

Received 30 April 2006; received in revised form 16 July 2006; accepted 28 July 2006
Available online 31 October 2006

Abstract

SiO_2 nanotubes (NTS) of different wall thickness were prepared using fibres of $[Pt(NH_3)_4][HCO_3)_2$ salt crystals. During growth of the SiO_2 nanotube walls by sol–gel condensation from tetraethyl orthosilicate (TEOS) on the surface of the templating Pt–salt fibres parts of the salt nanocrystals are incorporated into the walls due to strong SiO_2–salt interaction. This leads to a significant softening in the vibration density of states (VDS) of SiO_2. With increasing thickness of the SiO_2 NT walls the degree of Pt–salt incorporation decreases and consequently the observed shifting of IR Si–O vibration bands is more pronounced for NTs with thinner walls. In all cases the VDS relaxes during calcinations to those of pure SiO_2. Calcination leads to the formation of Pt nanoparticles and micropores within the nanotube walls.

Keywords: Oxide nanotubes; Pt nanoparticles; Templating Pt–salt; Calcination; IR spectroscopy

1. Introduction

Composites based on nanotubes (NTs) constitute a fascinating class of materials. Inspired by the discovery of carbon nanotubes in 1991 [1], also a large number of non-carbon NTs has been successively synthesized, e.g. from BN, GaN, ZnS or WS_2 [2–5] and oxides such as Al_2O_3, V_2O_5, SiO_2, TiO_2, SnO_2, ZrO_2 and MoO_3. An overview on oxide nanotubes was published by Patzke et al. [6]. Compared to carbon nanotubes the metallic and semiconductor properties of the different inorganic NTs often can be better controlled [7].

Template- and surfactant-aided reactions opened new doors into the fabrication of these nanotubes. For example, SiO_2 NTs with tube diameters below 10 nm were created with templates like cylindrical micelles of alkyl ammonium salts [8] or self-assembled fibril peptides [9]. However, most of the reported nanotubes are non-doped, and filling with doping compounds must be performed in a subsequent step.

Moreover, nanowhiskers or nanofibres (NFs) of different materials were synthesized e.g. from inverse microemulsions [10], by physical vapour deposition [11] or by sonochemical methods [12]. The nanowhiskers, nanofibres or nanowires can be used as structure-directing agents for the preparation of oxide nanotubes, e.g. uniform 30–40 nm thick silver nanowires were homogeneously coated with SiO_2 shells [13]. It was also proven that a fibrous metal oxide, $V_3O_7 \cdot H_2O$, can act as a template structure to get SiO_2 NTs which are 50–300 nm in diameter [14].

An alternative synthesis method to form metal doped SiO_2 or TiO_2 NTs employing metal–salt–nanofibres as templating structures was firstly established by our group. By this route e.g. Pt, Pd, Cu or Co doped oxide nanotubes have been synthesized so far [15,16]. A typical synthetic procedure is exemplarily drawn for Pt/SiO_2 NTs in Fig. 1. At first, template nanofibres (NFs) of amino-metal compounds, e.g. $[Pt(NH_3)_4][HCO_3)_2$, are prepared by solvent modification like addition of ethanol to an aqueous solution of the salt. After tailored precipitation of the

* Corresponding author. Tel./fax: +49 511 762 5298/19121.
E-mail address: michael.wark@pci.uni-hannover.de (M. Wark).

1387-1811/$ - see front matter © 2006 Elsevier Inc. All rights reserved.
doi:10.1016/j.micromeso.2006.07.032

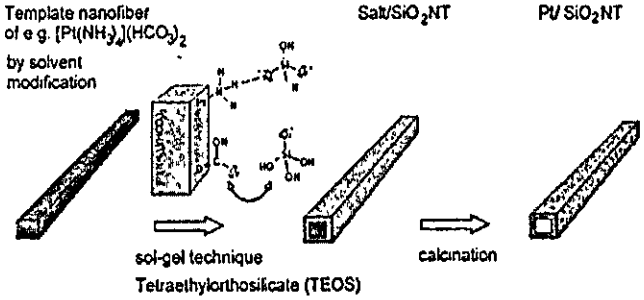

Fig. 1. Schematic illustration of the synthesis process of metal-containing SiO_2 NTs by the metal-salt–NF template method; the tubes are drawn open-ended for clarity.

Pt–salt crystals [17] a coating of the fibres by SiO_2 in a sol–gel process employing tetraethyl orthosilicate (TEOS) completes the composite synthesis. Subsequent calcination at 450 °C reduces the metal ions in the salt to metal clusters, which enter the porous SiO_2 walls or stay inside the tubes. In case of a Pt–salt to TEOS ratio of 1:5, which is the optimum to obtain exclusively NTs, a Pt content of 40 wt.% in the tubes is obtained [18]. In general, the obtained NTs mostly show close ends, although in Fig. 1 an open NT is drawn for clarity.

Strictly speaking the terms nanofibres (NFs) and nanotubes are somewhat misleading since the besides of the lengths also the fibre or tube diameters often exceed 100 nm. More correct would therefore sub-micrometer fibres or tubes but these terms are seldom used for structures of this kind and, thus, we also prefer to name them nanofibres and nanotubes.

Compared with others our metal–salt–NF template method is advantageous since it realises the preparation of SiO_2 NTs as well as their filling with metal nanoparticles simultaneously in an elegant and sufficient way. The easily achievable high amount of metal filling can provide many potential applications to the oxide NTs. Recently, catalytically active alumina and silica-alumina NTs with Pt particles hosted in their walls have been synthesized by this route [19,20]. A promising observation with respect to anisotropic electric conductivity is the formation of continuous Pt nanowires inside very thin SiO_2 or TiO_2 nanotubes [21]; titania NTs are prepared by employing tetrabutylorthotitanate (TBOT) instead of TEOS [15].

In order to tailor the composite nanotubes for specific applications the size and the localization of the Pt species is a crucial point. In some cases small particles in the nanotube walls are preferred, others require an unique arrangement of the metal, e.g. as nanowires or as chains of nanoparticles; the latter was found for magnetic Co nanoparticles in SiO_2 NTs [16], in the interior of the tubes. Recently, it has been shortly reported [22,23] that Pt–salt units can be bound tightly to the SiO_2 network leading to a strong shift in the SiO_2 related vibration density of states, which switches off during calcination. Here we present now more details concerning this interaction leading to a tailored uptake of Pt–salt units in the walls during the nanotube growth using temperature dependent IR spectroscopy, thermogravimetric (TGA) quantification, transmission electron microscopy (TEM) on thin slices of the NTs and N_2 adsorption determinations as characterizing methods.

2. Experimental

2.1. Controlled growth of monodisperse and ultralong Pt-containing SiO_2 NTs

Under a stirring rate of 300 rpm, 0.0125 mmol $[Pt(NH_3)_4](HCO_3)_2$ were dissolved in 1 mL ammonia, and then 0.7 mL ethanol were added into the solution. Afterward the system was kept inside an ice bath (ca. 0 °C) for at least 8 min, then 14 μL TEOS were added and the whole was again stirred for 2 min. With increased stirring rate of 1000 rpm, a small amount of ethanol was injected rapidly into the mixture and several minutes later the stirring rate was decreased to 300 rpm and 10 mL ethanol were added at a rate of 0.5 mL/min into the reaction system. Monodisperse and ultra long SiO_2 NTs were achieved after at most 4 h of stirring (sample Pt–NT1). When the addition of ethanol was finished, more TEOS could be added according to requirements [17]. In the case of sample Pt–NT2 another 28 μL TEOS have been added in order to get nanotubes with thicker walls. Thus the molar Pt:Si ratios have been 1:5 for Pt–NT1 and 1:15 for Pt–NT2, respectively.

After drying in air at room temperature, the samples were divided into several portions in order to use them in the different analysis techniques, i.e. temperature-dependent IR spectroscopy, thermogravimetric analysis and transmission electron microscopy on the non-calcined samples. The residues were calcined in air at 450 °C for 5 h (heating rate: 2 °C/min).

2.2. Characterization of non-calcined Pt–salt/SiO_2 nanotubes

For the different separated portions of the two charges of NTs, i.e. Pt–NT1 and Pt–NT2 with relatively thinner and thicker tube walls, respectively, calcination was done in thermogravemetry runs up to 500 °C (He as carrier gas, flow rate: 20 ml/min, heating rate: 5 K/min using a Setaram, Setsys evolution 1650 apparatus).

Temperature dependent IR (TIR) experiments were carried out in the same temperature range using KBr pellets in a specially designed furnace [24] directly in a FTIR device (Bruker IFS 66v).

Scanning electron microscopy (SEM) was made in secondary electron contrast at low excitation voltages in the range of 0.5 to 2 kV using a field-emission instrument of the type JEOL SM-6700 F.

TEM in absorption and phase contrast was made at 200 kV in a field-emission microscope of the type JEOL JEM-2100-F with an UHR pole piece that provided a

point-resolution better than 0.19 nm. Scanning transmission electron microscopy (STEM) was done in the same instrument employing bright-field (BF) and high-angle annular dark-field (HAADF) contrast.

Both, SEM and TEM were equipped with an ultrathin-window energy-dispersive X-ray spectrometer (EDXS) of the type Oxford Instruments INCA, respectively, that allowed elemental analysis.

Cross-sectional slices of the NTs were prepared in thicknesses of 30–50 nm by embedding powdery material in an Agar 100 resin and subsequent cutting with a diamond knife on an ultramicrotome of the type LKB 2128 Ultrotome IV. Finally, the thin slices have been fixed on 300 mesh copper grids.

3. Results and discussion

3.1. Formation of Pt–salt–nanofibres and SiO_2 nanotube tailoring

The formation of the templating $[Pt(NH_3)_4](HCO_3)_2$ nanofibres follows a procedure of nucleation and growth. Along with the drop wise addition of ethanol, in which the Pt–salt is practically insoluble, the Pt–salt in the aqueous solution is more and more concentrated and reaches the supersaturation state. Once the concentration of building blocks (ions) becomes sufficiently high, they aggregate into small clusters (nuclei) through a homogeneous nucleation. These nuclei serve as seeds for further anisotropic growth to form intermediate NFs (50–100 nm in diameter). From the careful analysis of the growth process of the $[Pt(NH_3)_4](HCO_3)_2$ nanofibres we elucidated a method for the formation of very uniform thin and long oxide nanotubes by employing TEOS, which prevents the aggregation among intermediately formed $[Pt(NH_3)_4](HCO_3)_2$ [17].

Under the adjusted basic conditions the hydrolysed TEOS species are partly deprotonated and, thus, negatively charged. They are able to exchange with some of the HCO_3^- ions on the surface of the $[Pt(NH_3)_4](HCO_3)_2$ nanofibres. Furthermore, they interact with the NH_3 ligands of the $[Pt(NH_3)_4]^{2+}$ complexes at the surface of the crystals via hydrogen bonds (compare Fig. 1). Both effects lead to an anchoring on the surface of the $[Pt(NH_3)_4](HCO_3)_2$ nanofibres. With the anchored silicate species as nucleation centres the SiO_2 walls are built-up by condensation processes. However, the silicate species attach preferentially on the slower growing side walls of the Pt salt nanofibres. The fast growing ends remain free and more $[Pt(NH_3)_4](HCO_3)_2$ nuclei of the solution can adsorb here. This promotes the anisotropic growth of the nanofibres.

After finalizing the whole TEOS addition and thus the sol–gel condensation process, highly anisotropic composites of $[Pt(NH_3)_4](HCO_3)_2$ nanofibres coated with a shell of SiO_2 result. The composite fibres exhibit aspect (length to width) ratios up to 800 (Fig. 2).

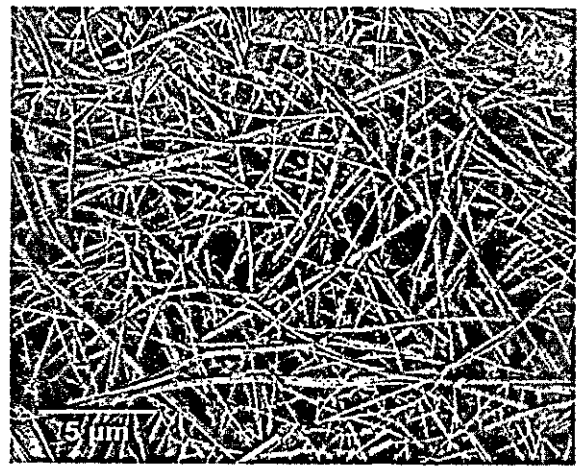

Fig. 2. Secondary electron micrograph revealing high aspect ratios up to 800 for the $[Pt(NH_3)_4](HCO_3)_2/SiO_2$ composite nanotubes.

3.2. Calcination of the Pt–salt/SiO_2 NT composites, formation of Pt metal clusters

The formation of the metal clusters in the nanocomposites can either be induced by electron bombardment or by auto-reduction in a heat treatment. In a transmission electron microscope the electron induced growth of Pt nanoparticles can be observed in-situ (Fig. 3A and B). Obviously, the reduction mainly starts at the boundary between the Pt salt and the SiO_2 walls. Here, already after some seconds of electron bombardment black spots and lines indicating the formation of electron-rich metallic Pt become visible in bright-field transmission electron micrographs (Fig. 3A). With progressing reduction, i.e. longer electron bombardment, the Pt metal structures grow to Pt nanoparticles mainly located on the inner SiO_2 wall (Fig. 3B).

After ex-situ heat treatment with air, however, the situation is different. Small 1–3 nm Pt nanoparticles are located in the porous SiO_2 walls whereas larger particles are again found close to the interior large pore of the formed nanotubes (Fig. 3C) [21]. Pt-doped SiO_2 nanotubes are formed, since during heat treatment the Pt salt decomposes according to the reaction (1):

$$[Pt(NH_3)_4](HCO_3)_2 \rightarrow Pt + 2N_2 + 5H_2 + 2CO_2 + 2H_2O \quad (1)$$

The formation of H_2 induces an autocatalytic process leading to the reduction of the Pt^{2+} ions; the gases N_2, CO_2, H_2O as well as NH_3, which might also be separated, released through the porous NT walls.

Since no Pt particles have been found on the external surface of SiO_2 nanotubes a migration of the formed Pt particles into the walls is not very likely. Such a Pt migration through the walls of the SiO_2 nanotubes is only possible in more reductive atmospheres (H_2); in this case higher amounts of Pt nanoparticles at the external surface have been observed [18]. In an oxygen containing atmosphere

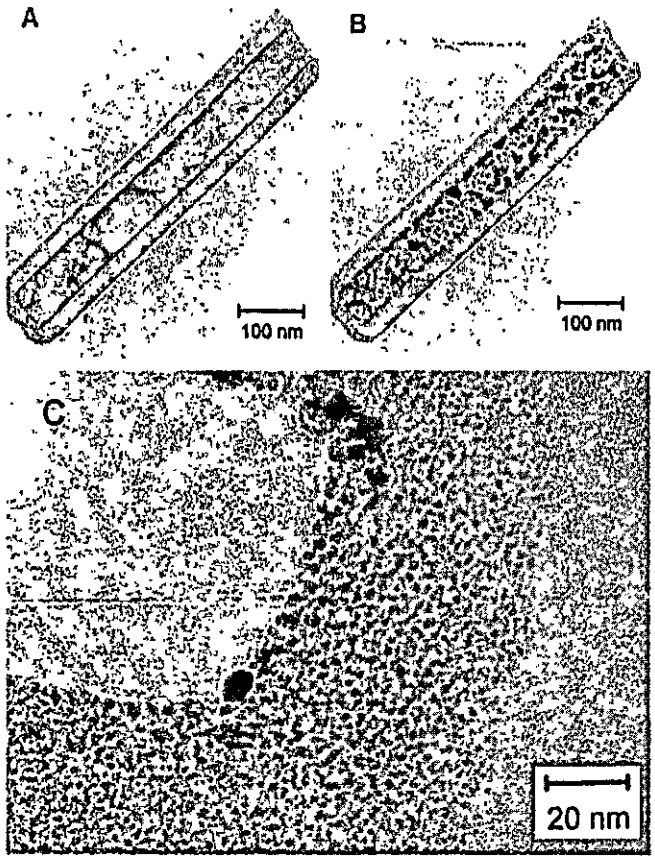

Fig. 3. Pt nanoparticles formed during the reduction of Pt–salt nanofibres in SiO_2 nanotubes; reduction induced by either bombardment with 120 keV electrons for 30 s (A) and 3 min (B), respectively or by calcination (450 °C, 5 h in stream of air) (C). The closer view into the porous walls in (C) shows Pt nanoparticles either penetrated into or directly formed in the walls.

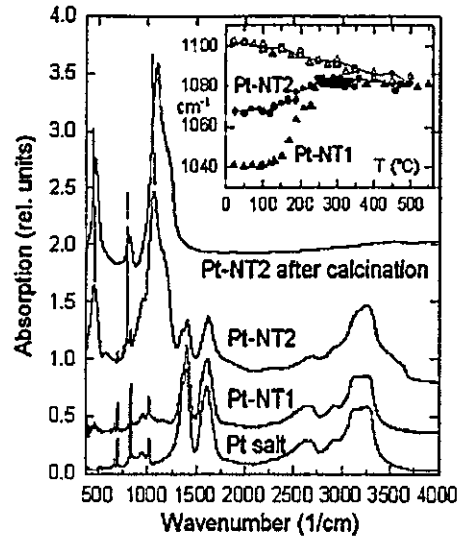

Fig. 4. IR spectra (in KBr) of samples as denoted (see text). The inset shows the shift of the main SiO_2 related peak maximum in the TIR experiments.

the Pt or Pt-oxo species strongly interact with the SiO_2 and are thus quite immobile. Also for the reduction of $[Pt(NH_3)_4]^{2+}$ salts in the pores of zeolites the smallest Pt nanoparticles, were found if heat treatment in an O_2 atmosphere was used [25]. This also indicates low diffusivity of Pt-oxo species.

An indication why nevertheless Pt nanoparticles were found in the walls after heat treatment in air is given by IR spectroscopy results on non-calcined $[Pt(NH_3)_4](HCO_3)_2$ nanofibres containing SiO_2 nanotubes.

The infrared absorption of two different charges of nanotube composites, i.e. with average NT widths of ca. 180 nm (Pt–NT1) and 400 nm (Pt–NT2) and SiO_2 walls of about 50 nm (Pt–NT1) and 180 nm (Pt–NT2) thickness, respectively, were measured before and after calcination in comparison to the pure Pt-salt (Fig. 4). Around 1500 cm^{-1} the spectra of the Pt-salt and the composites show two peaks resulting from N–H vibrations of the NH_3 ligands. The intensity of these peaks is lower for Pt–NT2, the sample with the thicker tube walls. In contrast to sample Pt–NT1, in which the Si–O vibrations of the SiO_2 walls around 400 cm^{-1} and 1200 cm^{-1} are much less intense, strong Si–O vibration signals are found in the sample Pt–NT2 with the thick walls. After heat treatment of both composites to 500 °C (in Fig. 4 only the spectra of calcined Pt–NT2 is shown) the N–H vibrations are completely disappeared and for the Si–O vibrations an irreversible shift to higher wavenumbers is found.

From TGA measurements (Fig. 5) the composition of the composites can be analysed quantitatively. For the pure salt a total weight loss of about 50 wt% occurs in one characteristic main step at the decomposition temperature of the salt at about 220 °C and is finished at around 300 °C. The weight loss perfectly corresponds to the decomposition of NH_3, CO_2 and H_2O from the Pt–salt nanofibres, since 49.4 wt.% of the mass of the Pt–salt result from Pt. The same characteristics were also observed for the composite materials. However, there are additional gradual losses below and above this temperature which are more significant for sample Pt–NT2 with the thicker SiO_2 walls indicating that these losses are related to water loss and condensation processes within the amorphous SiO_2. The detailed analysis of the TG curves reveals that the Pt–salt contribution in Pt–NT2 is about 28 wt.%, i.e. the SiO_2 contributes to about 72 wt.%. The loss of water from this SiO_2 part is responsible for the mass losses observed below and above the temperature range of 180–330 °C in which the Pt–salt decomposes. The same analysis for Pt–NT1 results in 76 wt.% contribution of Pt–salt, while only about 24% of the observed total weight loss results from the SiO_2 part. Thus the weight losses above and below 180–330 °C are much less pronounced than in Pt–NT2.

The most important IR finding, however, is related to the peak positions of the Si–O vibrations. At room temperature for the main Si–O related vibration maxima were found at about 1040 cm^{-1} and 1065 cm^{-1} in the non-calcined composite samples Pt–NT1 and Pt–NT2, respectively

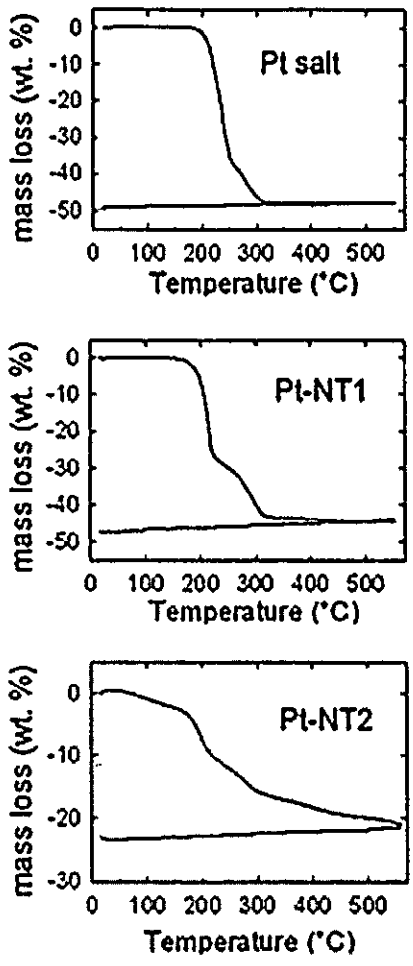

Fig. 5. Mass loss of the pure $[Pt(NH_3)_4](HCO_3)_2$ salt and the Pt-salt/SiO_2 nanotube composites Pt–NT1 and Pt–NT2 during thermogravimetric analysis.

(inset of Fig. 4). For amorphous SiO_2 the maximum of the Si–O vibration typically lies at 1100 cm^{-1} [24]. This value is also found for the composites after heating to 500 °C and cooling down to room temperature again, when the autoreduction took place and Pt nanoparticles containing SiO_2 nanotubes result. The quasi linear increase in frequency observed in the cooling curves of the NTs resembles that of pure SiO_2 glass indicating that calcination forms a largely relaxed SiO_2 network. After this first run the behaviour in successive cooling and heating runs always follow those of amorphous (dry) SiO_2 showing a slight decrease of the maximum wavenumber to 1080 cm^{-1} for high temperatures. For the other SiO_2 related peaks around 800 and 400 cm^{-1} quite analogous shifts were found.

The strong room temperature shifts of the SiO_2 related peaks of up to 60 wavenumbers in sample Pt–NT1 cannot only be explained by a strain effect via contact at the interface of the Pt-salt crystal inside the tube to the wall. The shifts of the Si–O vibrations to lower wavenumbers in the presence of the $[Pt(NH_3)_4](HCO_3)_2$ is clearly related to a strong interaction between the Pt-salt and the SiO_2 walls which becomes also obvious by the fact that the SiO_2 vibrations frequency is more lowered for the thinner wall NTs. This effect is explained by a higher effective density of salt type units incorporated in thinner wall NTs compared to thicker ones. In thicker walls the concentration of Pt-salt particles incorporated shows a significant gradient decreasing from the interior of the tubes towards the outer surface (compare Fig. 3C). Accordingly, the density of state peak maximum of SiO_2 related vibration is seen to be less much shifted in the thicker wall NTs.

These results imply that the templating Pt-salt nanofibres are already partially destructed during the coating with SiO_2 at room temperature and that Pt-salt type fragments of the nanocrystals are incorporated in the sol–gel grown SiO_2 walls due to strong Pt–O–Si interaction. The Pt gradient in the walls is well understandable because the dissolution of Pt-salt nanocrystals from the salt nanofibres will be most pronounced if the first layers of the SiO_2 coating are formed. If the thickness of the SiO_2 layer exceeds a critical thickness additionally attached TEOS will have no longer any influence on the underlying $[Pt(NH_3)_4](HCO_3)_2$ nanofibres.

Electron microscopy studies confirmed the presence of Pt species in the walls already prior to calcination. Fig. 6 shows a STEM annular dark-field micrograph, an EDX spectrum and an EDX mapping for Pt taken from the tube wall in an ultramicrotome slice of sample Pt–NT1. The EDX spectrum clearly shows Pt-M_β, Pt-L_l and Pt-L_α X-ray lines at about 2.1, 8.3 and 9.44 keV, respectively. Some parasitic Cu-L, -K_α, and -K_β signals at 0.93, 8.05, and 8.9 keV, respectively, are present due to fluorescent radiation from the supporting grid. The noncalcined SiO_2 nanotube still containing the templating $[Pt(NH_3)_4](HCO_3)_2$ salt was cut into thin slices by ultramicrotomy after being embedded in a resin. During this procedure the interior of the nanotube became accessible to the environment, and consequently all the Pt-salt inside the tube is dissolved. The Pt signal in the EDX spectrum results from Pt species which are grafted to or embedded in the walls by interaction with the silica; the distribution of Pt all over the walls is clearly visible from the EDX mapping taken at the Pt-M_β X-ray energy. In the STEM annular dark-field micrograph the Pt-salt nanocrystals are observed as bright white spots due to their higher electron scattering than the surrounding SiO_2.

For sample Pt–NT2 with thicker walls also Pt was found in the walls, but here the particles are more concentrated to the tube interior, like it is also seen in Fig. 3C.

3.3. Porosity of the Pt/SiO_2 NT walls

The formed walls of the SiO_2 nanotubes are highly porous. N_2 adsorption isotherms (Fig. 7) document that micropores, mesopores and macropores are present in sample Pt–NT1. The pore volume strongly increases during calcination; especially the number of micropores smaller than 2 nm in diameter in which N_2 adsorbs already at low relative pressure becomes more prominent. By applying the

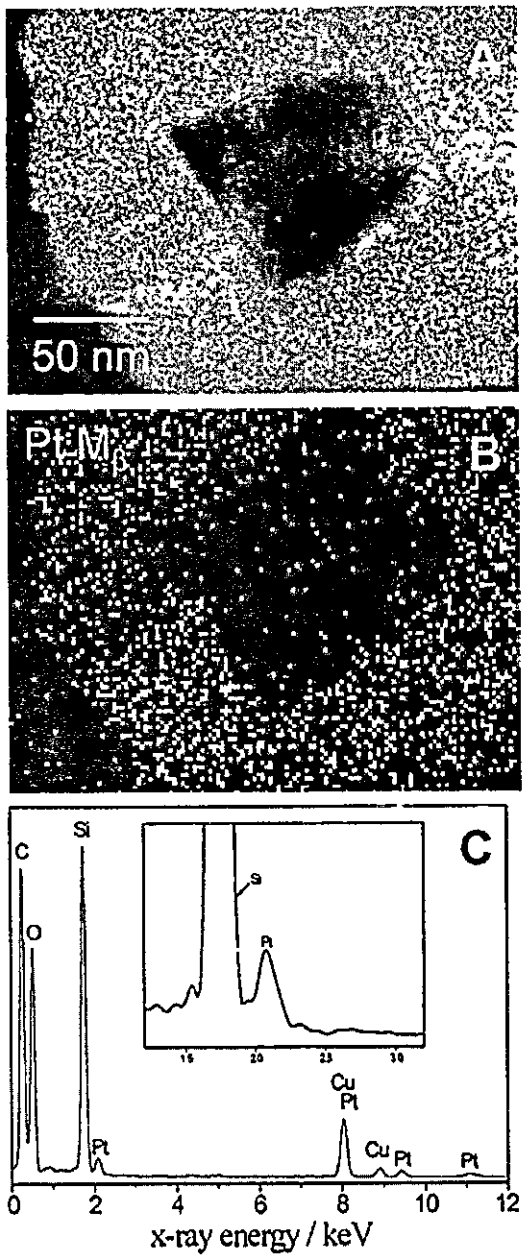

Fig. 6. Cross-sectional view of a non-calcined $[Pt(NH_3)_4](HCO_3)_2/SiO_2$ nanotube from sample Pt–NT1 by annular dark-field scanning transmission electron microscopy (A). The nanotube was embedded in a resin, and with an ultramicrotome, a thin slice of the sample was prepared. The bright dots observable in the tube walls result from highly electron scattering Pt atoms. EDX mapping of the same region with the Pt-M_β X-ray line (B); the Pt nanoparticles are visible as bright and grey spots in the walls. The EDX spectrum clearly confirms the presence of Pt species (C).

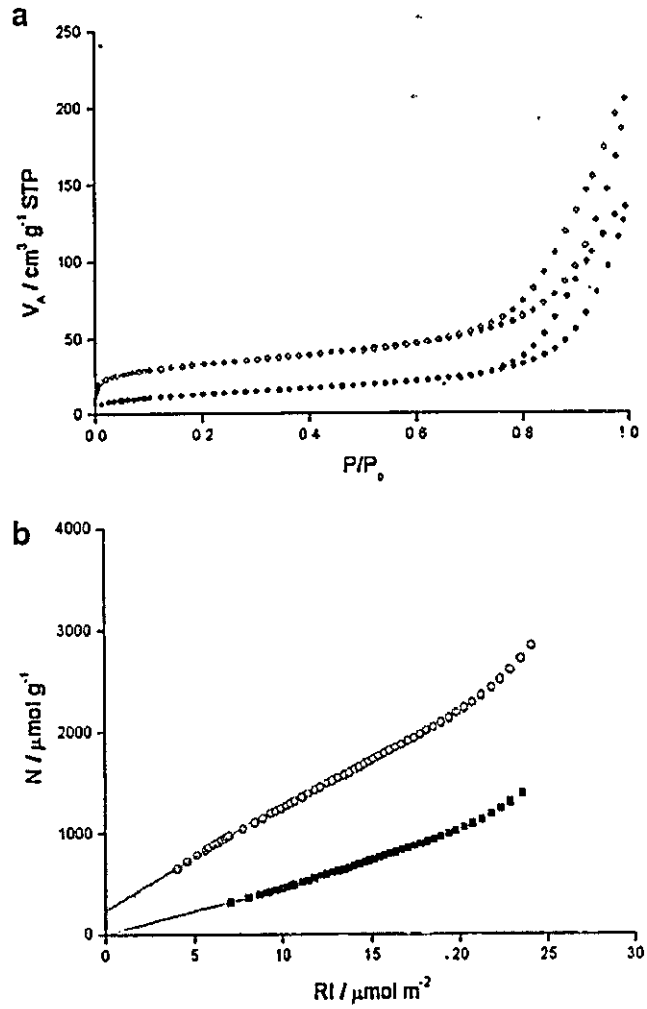

Fig. 7. N_2 adsorption/desorption isotherms of sample Pt–NT1 prior (full symbols) and after (open symbols) calcination in air at 450 °C (a). *t*–Plot of the N_2 adsorption data of Pt–NT1 in comparison to a non-porous SiO_2 reference material (b).

BET equation to the adsorption isotherms, the specific surface area of the degassed sample (treated for 16 h at 200 °C in order to remove all the adsorbed water) and of the calcined sample (air, 450 °C, 5 h, heating rate: 2 °C/min) were calculated to 48 m^2/g and 116 m^2/g, respectively, documenting an increase of about 150% due to calcination. The existence of micropores is proven by plotting the adsorbed amount of N_2 in calcined Pt–NT1 in relation to a N_2 adsorption on a non-porous SiO_2 reference material (right part of Fig. 7). The obtained linear fit intersects the ordinate at about 230 µmol/g; from this value a micropore volume of about 0.008 cm^3/g can be calculated. For Pt–NT2 the calcination induced increase in the micropore volume is less pronounced (about 70%) because, as already be concluded from the IR results, relatively less Pt is present in the thicker walls.

The diameters of the mesopores in the walls of the calcined NTs in sample Pt–NT1, as estimated by the BJH method, are ranging mostly between 3 and 10 nm. The hollow cavities of the NTs with diameters of around 50–70 nm act like macropores; their determination is beyond the applicability to the N_2 adsorption and the BJH method. Also the non-calcined sample turned from white to black during degassing at 200 °C for 16 h prior to the N_2 adsorption. This indicates that at least a part of the templating $[Pt(NH_3)_4](HCO_3)_2$ nanocrystals was already decomposed and reduced during the degassing treatment. The increased micropore volume and specific surface area of the sample after the calcination can be attributed to the creation of

small pores in the SiO_2 walls due to the destruction of the $[Pt(NH_3)_4](HCO_3)_2$ nanocrystals hosted in the tube walls and the formation of Pt nanoparticles in the walls. The creation of micropores or their enlargement due to a growth of Pt particles via Ostwald ripening is also well known from zeolite-based composites [26].

4. Conclusions

In order to form oxide nanotubes with several μm length precipitated $[Pt(NH_3)_4](HCO_3)_2$ nanofibres can be used as template structures and be coated with metal alkoxides in a sol–gel process. IR spectroscopy, electron microscopy and EDX results suggest that the structure-directing Pt nanofibres start to dissolve already during the sol–gel coating of the fibres with silica. A strong Pt–O–Si interaction might be responsible for the partial decomposition of salt fragments from the surface of the large Pt–salt–nanofibres.

Due to calcination in air the Pt–salt–template nanofibres as well as the salt nanocrystals split off and incorporated into the walls are reduced to Pt nanoparticles. The destruction of the salt crystals in the walls additionally creates micropores rendering these composites attractive for catalytic applications.

Acknowledgements

The authors thank Dr. J. Rathousky (Heyrovsky Institute of Physical Chemistry in Prague) for taking the N_2 adsorption isotherms and Prof. Dr. Jürgen Caro (Institute of Physical Chemistry, University of Hannover) for fruitful discussions. Financial support from the Deutsche Forschungsgemeinschaft (DFG, WA 1116-8) in the frame of the priority program SPP 1165 "Nanowires and nanotubes" is gratefully acknowledged.

References

[1] S. Iijima, Nature 363 (1991) 603.
[2] W. Tremel, Angew. Chem. Int. Ed. 38 (1999) 2175, and references therein.
[3] X. Wang, P. Gao, J. Li, C.J. Summers, Z.L. Wang, Adv. Mater. 14 (2002) 1732.
[4] J. Goldberger, R. He, Y. Zhang, S. Lee, H. Han, H.-J. Choi, P. Yang, Nature 422 (2003) 599.
[5] K.F. Huo, Z. Hu, J.J. Fu, H. Xu, X.Z. Wang, Y. Chen, Y.N. Lü, J. Phys. Chem. B 107 (2003) 11316.
[6] G.R. Patzke, F. Krumeich, R. Nesper, Angew. Chem. Int. Ed. 41 (2002) 2446.
[7] D. Appell, Nature 419 (2002) 553.
[8] M. Harada, M. Adachi, Adv. Mater. 12 (2000) 839.
[9] J.E. Meegan, A. Aggeli, N. Boden, R. Brydson, A.P. Brown, L. Carrick, A.R. Brough, A. Hussain, R.J. Ansell, Adv. Funct. Mater. 14 (2004) 31.
[10] Y. Liu, C. Zheng, W. Wang, C. Yin, G. Wang, Adv. Mater. 13 (2001) 1883.
[11] H. Yumoto, T. Sako, Y. Gotoh, K. Nishiyama, T. Kaneko, J. Cryst. Growth 203 (1999) 136.
[12] H. Wang, J.J. Zhu, J.M. Zhu, H.Y. Chen, J. Phys, Chem. B 106 (2002) 3848.
[13] Y. Yin, Y. Lu, Y. Sun, Y. Xia, Nano Lett. 2 (2002) 427.
[14] J. Zygmunt, F. Krumeich, R. Nesper, Adv. Mater. 15 (2003) 1538.
[15] C. Hippe, M. Wark, E. Lork, G. Schulz-Ekloff, Micropor. Mesopor. Mater. 31 (1999) 235.
[16] L. Ren, L. Guo, M. Wark, Y. Hou, Appl. Phys. Lett. 87 (2005) 212503.
[17] L. Ren, M. Wark, Chem. Mater. 17 (2005) 5928.
[18] M. Wark, C. Hippe, G. Schulz-Ekloff, Nanoporous materials II, in: A. Sayari, M. Jaroniec, T.J. Pinnavaia, (Eds.), Stud. Surf. Sci. Catal. 129 (2000) 475.
[19] T. Miyao, T. Saika, Y. Saito, S. Naito, J. Mater. Sci. Lett. 22 (2003) 543.
[20] Y. Sato, M. Koizumi, T. Miyao, S. Naito, Catal. Today 111 (2006) 164.
[21] F. Krumeich, M. Wark, L. Ren, H.-J. Muhr, R. Nesper, Z. Anorg. Allg. Chem. 630 (2004) 1054.
[22] C.H. Rüscher, L. Ren, M. Wark, Z. Krist. Suppl. 22 (2005) 94.
[23] C.H. Rüscher, A. Fiege, L. Ren, M. Wark, A. Feldhoff, 18. Deutsche Zeolithtagung, Book of abstracts, 2006, p. 46.
[24] C.H. Rüscher, Micropor. Mesopor. Mater. 86 (2005) 58.
[25] D. Exner, N. Jaeger, A. Kleine, G. Schulz-Ekloff, J. Chem. Soc. Faraday Trans. I 84 (1988) 4097.
[26] G. Schulz-Ekloff, in: P.A. Jacobs, N.I. Jaeger, L. Kubelkova, B. Wichterlova (Eds.), Zeolite Chemistry and Catalysis, Stud. Surf. Sci. Catal., vol. 69, Elsevier, Amsterdam, 1991, p. 65.